Biomedicine & Pharmacotherapy 166 (2023) 115304

Contents lists available at ScienceDirect

Biomedicine & Pharmacotherapy

journal homepage: www.elsevier.com/locate/biopha

Pharmacokinetics of the KRAS^{G12C} inhibitor adagrasib is limited by CYP3A and ABCB1, and influenced by binding to mouse plasma carboxylesterase 1c

Nancy H.C. Loos [a], Irene A. Retmana [a,b], Jamie Rijmers [a], Yaogeng Wang [a], Changpei Gan [a], Maria C. Lebre [a], Rolf W. Sparidans [b], Jos H. Beijnen [a,c,d], Alfred H. Schinkel [a,*]

[a] The Netherlands Cancer Institute, Division of Pharmacology, Amsterdam, the Netherlands
[b] Utrecht University, Faculty of Science, Department of Pharmaceutical Sciences, Division of Pharmacology, Utrecht, the Netherlands
[c] Utrecht University, Faculty of Science, Department of Pharmaceutical Sciences, Division of Pharmacoepidemiology and Clinical Pharmacology, Utrecht, the Netherlands
[d] The Netherlands Cancer Institute, Division of Pharmacy and Pharmacology, Amsterdam, the Netherlands

ARTICLE INFO

Keywords:
Adagrasib
KRAS^{G12C} inhibitor
ABCB1/P-glycoprotein
ABCG2/Breast cancer resistance protein
Cytochrome P450 3A
Carboxylesterase 1

Chemical compounds studied in this article:
Adagrasib (PubChem CID: 138611145)
Elacridar HCl (PubChem CID: 170320)
Zosuquidar (PubChem CID: 153997)
Ko143 (PubChem CID: 10322450)

ABSTRACT

Adagrasib (Krazati™) is the second FDA-approved specific KRAS^{G12C} inhibitor for non-small cell lung cancer (NSCLC) patients harboring this mutation. The impact of the drug efflux transporters ABCB1 and ABCG2, and the drug-metabolizing enzymes CYP3A and carboxylesterase 1 (CES1) on the pharmacokinetics of oral adagrasib were studied using genetically modified mouse models. Adagrasib was potently transported by human ABCB1 and modestly by mouse Abcg2 *in vitro*. In *Abcb1a/b*$^{-/-}$ and *Abcb1a/b;Abcg2*$^{-/-}$ mice, the brain-to-plasma ratios were enhanced by 33- and 55-fold, respectively, compared to wild-type mice, whereas ratios in *Abcg2*$^{-/-}$ mice remained unchanged. The influence of ABC transporters was completely reversed by coadministration of the dual ABCB1/ABCG2 inhibitor elacridar, increasing the brain penetration in wild-type mice by 41-fold while no signs of acute CNS toxicity were observed. Tumor ABCB1 overexpression may thus confer adagrasib resistance. Whereas the ABC transporters did not affect adagrasib plasma exposure, CYP3A and Ces1 strongly impacted its apparent oral availability. The plasma $AUC_{0-8\ h}$ was significantly enhanced by 2.3-fold in *Cyp3a*$^{-/-}$ compared to wild-type mice, and subsequently 4.3-fold reduced in transgenic CYP3A4 mice, indicating substantial CYP3A-mediated metabolism. Adagrasib plasma exposure was strongly reduced in *Ces1*$^{-/-}$ compared to wild-type mice, but tissue exposure was slightly increased, suggesting that adagrasib binds to plasma Ces1c in mice and is perhaps metabolized by Ces1. This binding could complicate interpretation of mouse studies, especially since humans lack circulating CES1 enzyme(s). Our results may be useful to further optimize the clinical safety and efficacy of adagrasib, and give more insight into potential drug-drug interactions risks.

1. Introduction

Mutations in the Kirsten rat sarcoma viral oncogene homolog (KRAS) occur frequently and are often involved in the most life-threatening cancer types, such as pancreatic, colorectal, and lung cancer [1,2]. The most common individual mutation in lung cancer is the oncogenic driver mutation KRAS^{G12C}, accounting for 14% of lung adenocarcinomas, and it is associated with a poor prognosis [1–3]. In May 2021, the Food and Drug Administration (FDA) approved sotorasib (Lumakras™), a specific KRAS^{G12C} inhibitor for patients with locally advanced or metastatic non-small cell lung cancer (NSCLC) displaying this specific mutation and who are at least treated with one other systemic therapy

Abbreviations: ABC, ATP-binding cassette; ANOVA, analysis of variance; AUC, area under the plasma concentration-time curve; BBB, blood-brain barrier; BCRP/ABCG2, Breast Cancer Resistance Protein; BSA, bovine serum albumin; CES1, carboxylesterase 1c; C_{max}, peak plasma concentration; CYP, cytochrome P450; DMEM, Dulbecco's modified essential medium; DMSO, dimethyl sulfoxide; DPBS, Dulbecco's phosphate-buffered saline; FBS, fetal bovine serum; FDA, Food and Drug Administration; FVB, Friend Virus B; GDP, guanosine diphosphate; GSH, glutathione; GTP, guanosine triphosphate; KRAS, Kirsten rat sarcoma virus; LC-MS/MS, liquid chromatography-tandem mass spectrometry; MDCK-II, Madin-Darby Canine Kidney II; NSCLC, P-glycoprotein, non-small cell lung cancerP-gp/ABCB1/MDR1; SD, standard deviation; TEER, transepithelial electrical resistance; T_{max}, time to reach peak plasma concentration; Zos, zosuquidar.

* Correspondence to: Division of Pharmacology, The Netherlands Cancer Institute, Plesmanlaan 121, 1066 CX Amsterdam, the Netherlands.
E-mail address: a.schinkel@nki.nl (A.H. Schinkel).

https://doi.org/10.1016/j.biopha.2023.115304
Received 29 March 2023; Received in revised form 1 August 2023; Accepted 7 August 2023
Available online 14 August 2023

[4,5]. Recently, another selective KRAS^{G12C} inhibitor, adagrasib (MRTX849; Krazati™), entered (pre-)clinical investigation for the same indication and received accelerated FDA approval in December 2022 [6]. Adagrasib is an irreversible covalent inhibitor, which binds to the cysteine 12 residue in the switch II pocket of the KRAS-protein, thereby locking the protein in its inactive GDP-bound state [1,2]. Based on phase I and II clinical studies, adagrasib at a dose of 600 mg twice daily shows efficacy and a tolerable safety profile [7,8]. However, still much of the pharmacokinetic behavior of adagrasib is not publicly known, especially its tissue distribution and brain penetration profile.

It is of importance for clinicians to have insights into pharmacokinetic determinants, which can provide them knowledge about possible drug-drug interactions and about drug safety and efficacy [9,10]. These pharmacokinetics determinants encompass drug efflux and influx transporters, and drug metabolizing enzymes. Among the family of drug efflux transporters, the ATP-binding cassette (ABC) transporter family are widely studied. P-glycoprotein (P-gp/ABCB1) and Breast Cancer Resistance Protein (BCRP/ABCG2) are important members of the ABC transporter family, and both transporters have a broad substrate specificity [11]. They are expressed in luminal (apical) membranes of cells in different organs, such as the brain, liver, small intestine and kidney [12]. In the brain, these transporters fulfill an important role in limiting the brain penetration of substrate drugs, because ABCB1 and ABCG2 reside at the blood-brain-barrier (BBB) [13–15]. Restricted brain exposure may negatively affect drug efficacy against brain (micro-) metastases [16,17]. Especially in KRAS^{G12C} NSCLC, brain metastases are relatively common with an incidence around 50%, therefore the extent of brain penetration of adagrasib is important [18]. Furthermore, ABCB1 and ABCG2 can play a role in limiting the intestinal absorption and they can facilitate direct hepatic, intestinal of renal excretion of their substrate drugs [10,12,19]. According to the FDA approval documentation, adagrasib seems to be a substrate as well as an inhibitor of ABCB1, but it is still unknown to what extent [6].

Besides drug efflux transporters, drug-metabolizing enzymes can also affect the oral availability of their substrate drugs. Cytochrome P450 (CYP) enzymes are often involved in drug-drug interactions. An important member of the CYP superfamily is CYP3A4, which is abundant in the human liver and small intestine [20,21]. CYP3A4 has a wide substrate specificity and can therefore limit the oral bioavailability and overall systemic exposure of a broad range of drugs [21]. Genetic polymorphisms can result in a divergent range of inter- and intra-individual enzyme activity of CYP3A4, as can enzyme inhibition or induction by other compounds or drugs, which can lead to a variable drug exposure in patients [20–22]. Based on preliminary results of the clinical studies with adagrasib, it is known that adagrasib is metabolized by CYP3A4 [8]. Six oxidation metabolites have been identified, of which the two most abundant ones, M10 and M11, are pharmacodynamically active. However, the total circulating metabolite concentration only accounts for 15–30% of the total drug levels in plasma [8]. Although CYP3A4 can metabolize adagrasib based on human liver hepatocyte studies, these *in vitro* results are limited to liver CYP3A, whereas CYP3A4 is also highly abundant in the intestine. Therefore, we were interested in the broader *in vivo* metabolism of adagrasib in the liver and intestine. The FDA approval documentation further describes CYP3A inhibition by adagrasib [6].

The carboxylesterase 1 (CES1) enzyme complex can also influence the oral bioavailability of substrate drugs. CES1 is expressed in the human liver, small intestine and kidney, and able to hydrolyze many (but not all) carboxylic acid ester, amide and thioester bonds in substrate drugs [23–25]. CES1 is most abundant in the liver, mainly in the endoplasmic reticulum, and to a lesser extent in the kidney and adipose tissue. Interestingly, an important species difference between mice and humans is the predominant secretion of murine Ces1c from the liver into plasma, whereas human CES1, while highly expressed in the liver, is not secreted [25]. Moreover, the mouse has 8 Ces1 enzymes (Ces1a-h), whereas humans have only one mature CES1 protein isoform encoded by one or two closely related genes. In view of the presence of an amide bond in adagrasib (Suppl. Fig. 1), it might be hydrolyzed by the Ces1 enzyme(s), or it might be bound by them.

In the current study, we wanted to gain more insight into the impact of ABCB1 and ABCG2 efflux transporters, as well as the drug-metabolizing enzymes CYP3A and CES1 on the plasma pharmacokinetics and tissue distribution of adagrasib. For this purpose, we studied oral adagrasib pharmacokinetics in Abcb1 and Abcg2 knockout mouse strains, and Ces1 and Cyp3a knockout mice, including a humanized CYP3A4 transgenic mouse model.

2. Materials and methods

2.1. Chemicals

Adagrasib (MRTX849) was obtained from MedKoo Biosciences (Morrisville, NC). Zosuquidar (Zos) was purchased from Sequoia Research Products (Pangbourne, United Kingdom) and Ko143 from Tocris Bioscience (Abingdon, United Kingdom). Elacridar HCl was supplied by Biosynth (Bratislava, Slovakia). Bovine Serum Albumin (BSA) Fraction V was obtained from Roche Diagnostics (Mannheim, Germany). Glucose water (5%, w/v) was purchased from B. Braun Medical Supplies (Melsungen, Germany). Isoflurane was supplied by Virbac Nederland (Barneveld, The Netherlands) and heparin (5000 IU·mL^{-1}) from Leo Pharma (Breda, The Netherlands). Other chemicals and reagents needed for the assay of adagrasib were described before (manuscript submitted). All other reagents and chemicals that were used, were obtained from Sigma-Aldrich (Steinheim, Germany).

For the cell culture prior to the transwell experiments, Dulbecco's Modified Essential Medium (DMEM) glutamax, penicillin-streptomycin 10,000 U/L, and Dulbecco's Phosphate-Buffered saline (DPBS) were supplied by Life Technologies (Bleiswijk, The Netherlands). Fetal Bovine Serum (FBS) was purchased from Serana (Pessin, Germany).

2.2. Cell lines

The cell lines used in the drug transporter assay were parental Madin–Darby Canine Kidney cells (MDCK-II, European Collection of Cell Cultures, ECACC 00062107) and stably transduced subclones with human (h) ABCB1, hABCG2, or mouse (m) Abcg2 cDNA. These cell lines were grown at 37 °C in 5% CO_2 and all were mycoplasma free [26–28]. Supplemented culture medium (DMEM with 10% (v/v) FBS and 1% (v/v) of penicillin-streptomycin stock) was used to culture these cell lines. Prior to the drug transport assay, the different cell lines were cultured for at least 2 weeks. The passage numbers of the cells used for the transport assay ranged between 10 and 15.

2.3. Drug transporter assay

For the *in vitro* transepithelial drug transport assays 12-well plates with microporous polycarbonate membrane filter inserts (3.0-μm pore size, 12-mm diameter, Transwell 3402, Corning; Amsterdam, The Netherlands) were used. The parental MDCK-II cells and the transduced subclones were seeded at a density of 2.5×10^5 cells per well. Prior to the transport assay, the cells were cultured for 3 days to guarantee the formation of an intact monolayer. The culture medium was replaced one and two days after seeding the cells. Before the start of the drug transport assay and afterwards, the transepithelial electrical resistance (TEER) levels were measured to confirm the integrity of the monolayer membranes. During the experiment all TEER values met the reference levels ($\geq$ 70 Ω·cm^2 for the parental and hABCG2-overexpressing, $\geq$ 200 Ω·cm^2 for the hABCB1-overexpressing, and $\geq$ 140 Ω·cm^2 for the mAbcg2-overexpressing cell line).

Adagrasib, zosuquidar (ABCB1 inhibitor) and Ko143 (ABCG2/Abcg2 inhibitor) were each dissolved in DMSO at a concentration of 2 mM, and further diluted 1000-fold with DMEM medium containing 10% (v/v)

FBS to obtain 2 μM working solutions. Prior to the drug transporter assay, the cell lines were preincubated with only medium or a mixture of medium with the inhibitor(s) in both compartments during 1 h. Subsequently, the transport phase was initiated (t = 0) by replacement of the medium in the donor compartment (either basolateral or apical) by fresh medium containing 10% FBS, 2 μM adagrasib and, where appropriate, 2 μM inhibitor(s), respectively. During the whole transport assay, the MDCK-II cells were kept at 37 °C, pH 7.4, in a 5% (v/v) CO_2 environment. At 1, 2, 4, and 8 h after the start of the assay, sample collection (50 μL) from the acceptor compartment was performed. The samples were stored at − 30 °C until further bioanalytical pretreatment and analysis. The transport ratio r was calculated to measure the active transport of adagrasib by dividing the degree of transport in the apical direction by the degree of transport in the basolateral direction after 8 h.

2.4. In vitro adagrasib plasma stability assay

Fresh plasma was collected from 3 to 6 wild-type and *Ces1*$^{-/-}$ mice, and independent triplicate incubations were set up in the absence or presence of 1 mM BNPP. After 15 min preincubation at 37 °C, adagrasib was spiked at a concentration of 2000 ng/mL and incubation was continued at 37 °C with vigorous shaking. At 0, 7.5, 15, 30, 60, 120, and 240 min, samples were taken and pipetted and mixed directly onto a 10 mM BNPP solution to a final concentration of 1 mM BNPP. Collected samples were kept on ice and snap-frozen after the last sample was taken. Adagrasib concentrations were measured as described under Section 2.9 below.

2.5. Animals

Mice were housed and handled according to institutional guidelines complying with Dutch and EU legislation. All experimental animal protocols (under national permit numbers AVD301002016595 and AVD30100202114776) used for this study, were approved by the institutional board for care and use of laboratory animals. Adagrasib was used in different pharmacokinetic studies using female wild-type, *Abcb1a/1b*$^{-/-}$, *Abcg2*$^{-/-}$, *Abcb1a/1b;Abcg2*$^{-/-}$, *Ces1*$^{-/-}$ (*Ces1* cluster knockout: *Ces1a-Ces1h*), *Cyp3a*$^{-/-}$, and Cyp3aXAV (overexpression of human CYP3A in liver and intestine of *Cyp3a*$^{-/-}$) mice. All animals were of a > 99% FVB genetic background, and their age was between 9 and 15 weeks. The housing conditions of the mice were specific pathogen-free, temperature-controlled and with a 12-hour light and 12-hour dark cycle. Mice received a standard diet (Transbreed, SDS Diets, Technilab-BMI, Someren, The Netherlands) and acidified water *ad libitum*. Animal welfare assessments were performed before, during, and after the experiments.

2.6. Oral drug solutions

Adagrasib was dissolved in DMSO at a concentration of 30 mg/mL, and further 10-fold diluted with polysorbate 80/ethanol (1:1, v/v), and 5% (w/v) glucose in water to yield an adagrasib concentration of 3 mg/mL in the dosing solution for oral administration [1:2:7, (v/v/v)]. Final vehicle concentrations were 10% v/v DMSO, 10% v/v polysorbate 80, 10% v/v ethanol, and 3.5% w/v glucose. For the boosting study, elacridar HCl was dissolved in DMSO at 53 mg/mL to obtain 50 mg elacridar base per mL. This stock solution was further diluted 10-fold with a mixture of polysorbate 80, ethanol and water [20:13:67 (v/v/v)], to yield an elacridar concentration of 5 mg/mL in the oral dosing solution. Final vehicle concentrations were 10% v/v DMSO, 18% v/v polysorbate 80, 11.7% v/v ethanol, and 60.3% v/v water. All dosing solutions were prepared freshly on the day of the experiment.

2.7. Plasma pharmacokinetics and tissue distribution of adagrasib in mice

Mice were fasted for 2–3 h before oral adagrasib administration to minimize variation in oral drug absorption. Adagrasib (30 mg/kg of body weight; 3 mg/mL dosing solution) was administered by oral gavage into the stomach using a blunt-ended needle. Female wild-type, *Abcb1a/1b*$^{-/-}$, *Abcg2*$^{-/-}$, *Abcb1a/1b;Abcg2*$^{-/-}$, and *Ces1*$^{-/-}$mice were used in a 2-hour experiment, and female wild-type, *Cyp3a*$^{-/-}$, and Cyp3aXAV (overexpression of human CYP3A in liver and intestine of *Cyp3a*$^{-/-}$) mice were used in an 8-hour experiment. Blood sampling via the tail vein (~50 μL per sample) using heparinized microvettes was performed at 5, 10, 15, 30, and 60 min after adagrasib administration for the 2-hour experiment. For the 8-hour experiment, the sampling time points were 0.0625, 0.125, 0.5, 1, 2, and 4 h after administration of adagrasib. At the final time point (2 or 8 h), mice were anesthetized using an isoflurane evaporator with 3% isoflurane with 0.8 L/min air and 0.3 L/min oxygen. A cardiac puncture was performed, and the final blood sample was collected using a heparinized needle and syringe. Subsequently, the anesthetized mice were sacrificed by cervical dislocation, and brain, liver, spleen, kidney, small intestine, and lungs were collected. The small intestinal content (SIC) was also separately collected by removing this from the small intestinal tissue, which was rinsed with saline to remove possible residual feces. Centrifugation at 9000 x g for 6 min at 4 °C was used to separate the plasma from the blood. All plasma fractions were stored at − 30 °C until analysis. Brain, liver, spleen, kidney, small intestinal tissue, SIC, and lung were homogenized in a FastPrep-24TM 5 G homogenizer (M.P. Biomedicals, Santa Ana, CA) for 1 min with 1, 3, 1, 2, 3, 2, and 1 mL of 2% (w/v) BSA, respectively. All tissue samples were stored at − 80 °C until analysis.

2.8. Adagrasib pharmacokinetic boosting study with orally administered elacridar

Three hours prior to the adagrasib administration, elacridar (50 mg/kg of body weight; 5 mg/mL dosing solution) or vehicle solution was orally administered to wild-type and *Abcb1a/1b;Abcg2*$^{-/-}$ mice. Subsequently, all mice were fasted for at least 3 h. After this fasting period, oral administration of adagrasib (30 mg/kg of body weight; 3 mg/mL dosing solution) was performed as described above. Tail vein blood sampling was performed at 5, 10, 15, and 30 min after administration of adagrasib. Termination of this boosting experiment was performed as described above by performing cardiac puncture under isoflurane anesthesia at 1 h after adagrasib administration. The same organs of interest were collected. All samples were processed and stored as described above.

2.9. Bioanalytical analysis

A recently developed specific and validated liquid chromatography-tandem mass spectrometry (LC-MS/MS) method was used to measure the concentrations of adagrasib in DMEM cell culture medium, plasma samples, and tissue homogenates (manuscript submitted).

2.10. Pharmacokinetic calculations and statistical analysis

Non-compartmental methods were used to calculate the pharmacokinetic parameters using the software package of PK solutions 2.0.2 (SUMMIT, Research Service, Montrose, CO). The linear trapezoidal rule without extrapolating to infinity was used to calculate the area under the curve (AUC) of adagrasib. The peak plasma concentration (C_{max}) and time of peak plasma concentration (T_{max}) were obtained from the raw data from each individual mouse. For the graph drawing and statistical analysis, GraphPad Prism 9 (GraphPad Software Inc., La Jolla, CA) was used. For the comparison of two groups, the two-sided unpaired Student t-test was applied. When multiple groups were compared, one-way analysis of variance (ANOVA) was performed, whereas Sidak's *post hoc* correction was applied to account for the multiple comparisons. In view of the often large differences in means and standard deviations between groups, data were first log-transformed before applying

statistical analysis. Differences were considered statistically significant, when $P < 0.05$. All data are presented as geometric mean ± SD.

3. Results

3.1. In vitro adagrasib transport assay in ABC-transporter transduced MDCK-II cells

The parental Madin-Darby Canine Kidney (MDCK-II) cell line and subclones overexpressing hABCB1, hABCG2, and mAbcg2 were used in a transepithelial drug transport assay to determine if adagrasib is a substrate for one of these drug transporters and to what extent it is transported. Adagrasib (2 μM) was modestly transported in the parental cell line (transport ratio r = 1.71, Fig. 1A) to the apical side of the membrane, which could be inhibited by the ABCB1 inhibitor zosuquidar (2 μM) (r = 1.03, Fig. 1B). Transport of adagrasib was efficient in the hABCB1 overexpressing cell line (r = 4.98, Fig. 1C), and this transport was also inhibited by zosuquidar (r = 1.33, Fig. 1D). The medium used for the hABCG2 and mAbcg2 overexpressing cells contained zosuquidar to avoid any transport contribution of canine Abcb1. In the MDCK-II-hABCG2 cells, there was little or no polarized transport or impact of the ABCG2 inhibitor Ko143 (r = 1.20 and r = 0.92, Fig. 1E-F). Apically directed transport of adagrasib was observed in the mAbcg2-overexpressing cell line (r = 3.31, Fig. 1G), which could be inhibited by Ko143 (r = 1.18, Fig. 1H). Adagrasib thus appears to be efficiently transported by hABCB1 and mAbcg2 *in vitro*, whereas hABCG2 showed no significant transport of adagrasib.

3.2. Adagrasib brain penetration is strongly restricted by Abcb1 and modestly by Abcg2

The potential impact of Abcb1 and Abcg2 on the pharmacokinetics and tissue distribution of adagrasib was studied in wild-type, *Abcb1a/1b*$^{-/-}$, *Abcg2*$^{-/-}$, and *Abcb1a/1b;Abcg2*$^{-/-}$ mice. Due to the lack of a recommended human dose at the time of these experiments, adagrasib was orally dosed based on the lowest effective dose (30 mg/kg) in limited tumor cell studies in mice [2]. Adagrasib was readily absorbed, with a T_{max} around 1 h (Fig. 2A). The plasma $AUC_{0–120\ min}$ was not significantly different between wild-type mice and the *Abcg2*$^{-/-}$ and *Abcb1a/1b;Abcg2*$^{-/-}$ mice (Fig. 2B, Suppl. Table 1), but reduced by 36% in the *Abcb1a/1b* knockout strain compared to wild-type mice ($P < 0.01$, Fig. 2B, Suppl. Table 1). The C_{max} was also lower in *Abcb1a/1b*$^{-/-}$ compared to wild-type and to *Abcg2*$^{-/-}$ mice ($P < 0.01$, Suppl. Table 1). However, overall it seems that the ABC transporters have only a slight, if any, impact on the plasma pharmacokinetics of adagrasib.

When the tissue disposition of adagrasib was assessed, in both *Abcb1a/1b*$^{-/-}$ and *Abcb1a/1b;Abcg2*$^{-/-}$ mice a strong enhancement of the brain-to-plasma ratio was observed compared to wild-type mice, by respectively 36- and 60-fold (both $P < 0.0001$, Fig. 2C-D, Suppl. Table 1). In the single *Abcg2*$^{-/-}$ mice, we did not observe any impact on the brain exposure of adagrasib. However, both transporters appear to contribute to the efflux of adagrasib from the brain, based on the significant, almost 2-fold increase in brain disposition in the combined ABC-transporter knockout strain compared to the single *Abcb1a/1b*$^{-/-}$ mice ($P < 0.01$, Fig. 2C-D, Suppl. Table 1). Another interesting finding was that the intrinsic brain exposure of adagrasib in wild-type mice was relatively low (brain-to-plasma ratio of 0.07), which could be disadvantageous for adagrasib efficacy against brain (micro-)metastases.

Other matrices potentially affected by the ABC transporters are the small intestine and the small intestinal content (SIC). For the latter, we mainly focus on the recovered percentage of the administered dose of adagrasib in SIC, as the often variable fecal matter content between individual mice can skew concentration data. The SIC % of dose was decreased in *Abcb1a/1b*$^{-/-}$ ($P < 0.05$) and *Abcb1a/1b;Abcg2*$^{-/-}$ mice, albeit not statistically significant in *Abcb1a/1b;Abcg2*$^{-/-}$ mice, compared to wild-type mice (Suppl. Fig. 2D, Suppl. Table 1). A similar pattern, but now significant for both strains, was observed when comparing them to *Abcg2*$^{-/-}$ mice (both $P < 0.01$, Suppl. Fig. 2D, Suppl. Table 1). In contrast, the small intestine tissue concentrations and the small intestine-to-plasma ratios did not show clear, meaningful differences between the different strains (Suppl. Fig. 2A-B). The reduced recovery of adagrasib in the SIC of both Abcb1a/1b-deficient strains could be related to hepatobiliary excretion of adagrasib or due to its active transport from the intestinal epithelium back into the intestinal lumen by Abcb1a/1b in wild-type mice, or a combination of both processes. A possible involvement of the Abcb1a/1b transporters in the hepatobiliary excretion of adagrasib could also be reflected in the liver-to-plasma ratios, which were slightly increased in the *Abcb1a/1b*$^{-/-}$ and *Abcb1a/1b;Abcg2*$^{-/-}$ compared to wild-type mice (Suppl. Fig. 3B). The kidney distribution appeared to be affected by both ABC transporters combined, as the kidney concentration and kidney-to-plasma ratios were significantly decreased in the *Abcb1a/1b;Abcg2*$^{-/-}$ mice compared to all the other strains ($P < 0.001–0.05$, Suppl. Fig. 3E and F). For the other analyzed tissues, no meaningful changes were observed in the different ABC transporter-deficient strains compared to wild-type mice (Suppl. Fig. 3).

3.3. Boosting adagrasib brain penetration with the ABCB1/ABCG2 inhibitor elacridar

We found that the intrinsic brain penetration of adagrasib is relatively low and that its brain disposition can be restricted by mAbcb1a/b and mAbcg2. This could be of clinical relevance, if the same applies to the human situation, because it might limit adagrasib efficacy against brain (micro-)metastases. Therefore, we assessed the influence of oral coadministration of the dual ABCB1/ABCG2 inhibitor elacridar on the brain disposition of adagrasib. We first administered elacridar (50 mg/kg) or vehicle solution to wild-type and *Abcb1a/1b;Abcg2*$^{-/-}$ mice 3 h prior to the oral administration of adagrasib to obtain maximal ABC transporter inhibition, as the T_{max} of elacridar is around 4 h. The experiment was terminated 1 h after adagrasib administration.

The plasma exposure of adagrasib ($AUC_{0–1\ h}$ and C_{max}) was not significantly altered between wild-type mice and *Abcb1a/1b;Abcg2*$^{-/-}$ in either the vehicle- or elacridar-pretreated groups (Fig. 3A-B, Suppl. Table 2). This is in accordance with the previous experiments. In contrast, we observed a pronounced impact of elacridar on the tissue disposition of adagrasib. There were strong increases in brain concentrations (45.5-fold, $P < 0.0001$) and brain-to-plasma ratios (41.0-fold, $P < 0.0001$) in wild-type mice pretreated with elacridar compared to vehicle (Fig. 3C-D). The levels obtained in the elacridar-treated group of the wild-type mice were even slightly higher, albeit not statistically significant, compared to *Abcb1a/1b;Abcg2*$^{-/-}$ with or without elacridar. Altogether, the data suggest complete inhibition of the ABCB1 and ABCG2 transporters in the BBB (Fig. 3C-D, Suppl. Table 2). Elacridar treatment had no significant effect in the *Abcb1a/1b;Abcg2*$^{-/-}$ mice (Fig. 3). It is further important to note that we observed no signs of acute CNS toxicity in any of the mice in this experiment.

The liver disposition of adagrasib also seemed to be slightly affected by the coadministration of elacridar: in both strains the liver concentrations were slightly increased compared to their vehicle groups ($P < 0.05$, Suppl. Fig. 4A). A similar pattern was observed for the kidney data (Suppl. Fig. 4E-F). As these shifts with limited significance occurred in both strains, perhaps this was caused by an effect of elacridar separate from its inhibition of ABCB1 and ABCG2. All the other analyzed tissues did not seem to be affected by the coadministration of elacridar in any of the strains (Suppl. Fig. 4).

3.4. CYP3A strongly restricts the plasma exposure of adagrasib

The influence of the primary drug-metabolizing enzyme complex CYP3A on the plasma exposure and tissue disposition of oral adagrasib was studied in an 8-hour experiment, using female wild-type, *Cyp3a*$^{-/-}$ and transgenic Cyp3aXAV mice (humanized mouse model consisting of

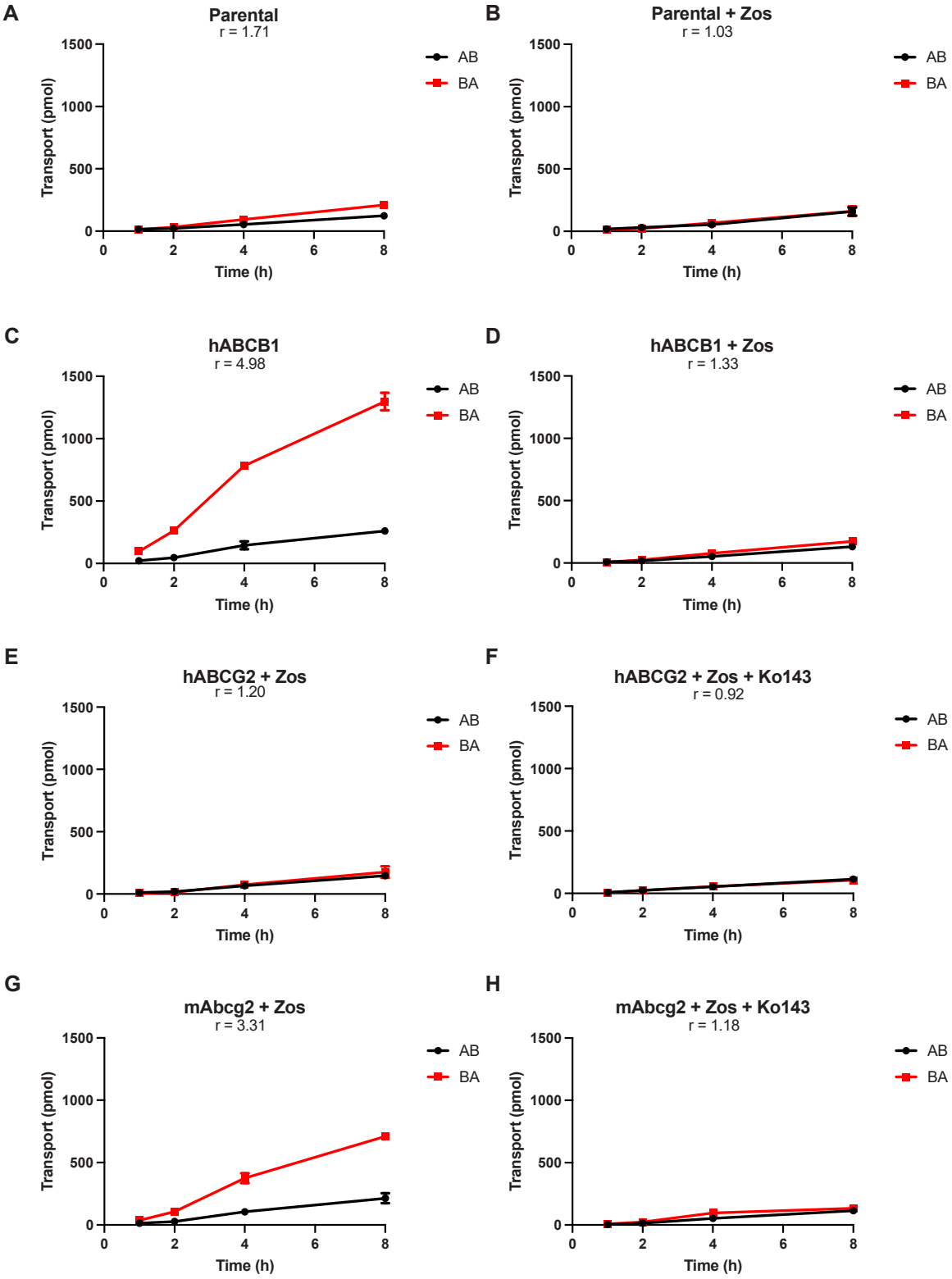

Fig. 1. Transepithelial transport of adagrasib (2 μM) in MDCK-II cells, either parental (A, B), transduced with hABCB1 (C, D), hABCG2 (E, F) or mAbcg2 (G, H) cDNA. At t = 0 h, adagrasib was added in the donor compartment, and concentrations were measured in the acceptor compartment at t = 1, 2, 4, and 8 h. Data are plotted as cumulative adagrasib transport (pmol) per well over time (n = 3). B, D–H: Zosuquidar (Zos, 2 μM) was added to inhibit human and/or endogenous canine Abcb1. F and H: the ABCG2 inhibitor Ko143 (2 μM) was used to inhibit ABCG2/Abcg2. r, relative *t*ransport ratio. BA (■), translocation from the basolateral to the apical compartment; AB (●), translocation from the apical to the basolateral compartment. Data are presented as mean ± SD.

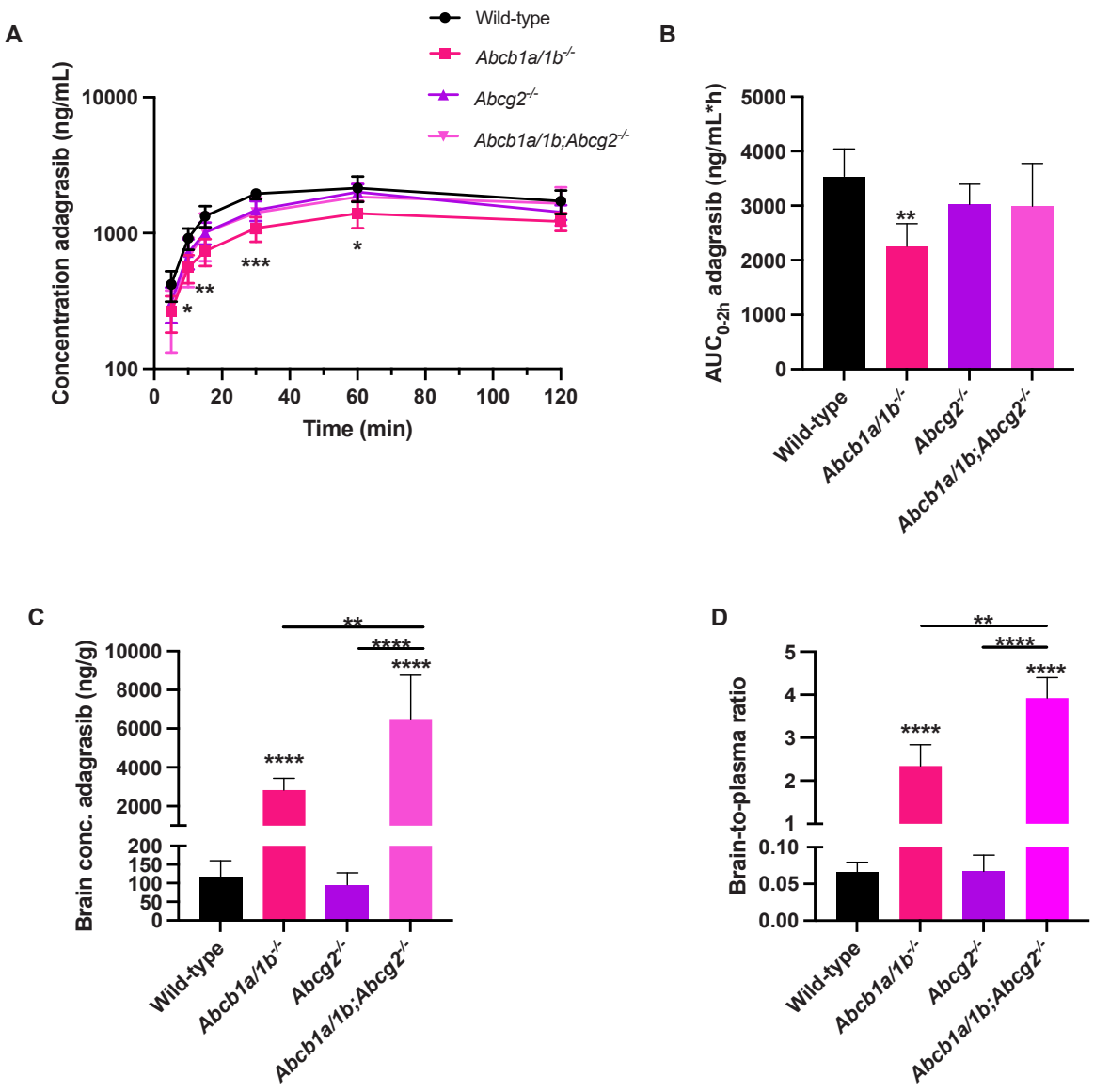

Fig. 2. Pharmacokinetic parameters of adagrasib (30 mg/kg) in female wild-type, *Abcb1a/1b*$^{-/-}$, *Abcg2*$^{-/-}$, and *Abcb1a/1b;Abcg2*$^{-/-}$ mice over 2 h after oral administration (n = 6). **A.** Plasma concentration time curve of adagrasib (semi-log scale). **B.** $AUC_{0-2\,h}$, area under the plasma concentration-time curve from 0 to the last time point (t = 2 h). **C.** Brain concentrations (ng/g). **D.** Brain-to-plasma ratios. Data are presented as mean ± SD. Panel A: * , $P < 0.05$; * *, $P < 0.01$; * ** , $P < 0.001$ *Abcb1a/1b*$^{-/-}$ compared to wild-type mice. No significant differences in plasma concentration were observed for any time point between wild-type and the other two strains. Panels B-D: * *, $P < 0.01$; * ** , $P < 0.001$; * ** *, $P < 0.0001$ compared to wild-type mice or another mouse strain as indicated by the bars.

Cyp3a deficient mice overexpressing transgenic human CYP3A4 in liver and small intestine). The C_{max} of adagrasib in wild-type mice occurred somewhat earlier than in *Cyp3a*$^{-/-}$ mice, with a T_{max} of 1.5 h compared to 3.3 h. Cyp3a appears to play a significant role in the plasma pharmacokinetics of adagrasib, because the $AUC_{0-8\,h}$ was enhanced by 2.3-fold and the C_{max} by 2.1-fold in the Cyp3a-deficient mouse strain compared to wild-type ($P < 0.0001$, Fig. 4, Suppl. Table 3). In the transgenic Cyp3aXAV mice the $AUC_{0-8\,h}$ and C_{max} were significantly reduced by 4.3- ($P < 0.0001$) and 3.7-fold ($P < 0.0001$), respectively, compared to *Cyp3a*$^{-/-}$ mice (Fig. 4B-C, Suppl. Table 3). Therefore, these results indicate that both mouse Cyp3a and human CYP3A4 are important players in the metabolism of adagrasib, significantly restricting its plasma exposure.

When studying the influence of Cyp3a and CYP3A4 on the tissue distribution of adagrasib, it is important to assess the tissue-to-plasma ratios as well as the absolute tissue concentrations, in view of the clear differences in plasma exposure between the three strains. CYP3A4 is most abundant in the liver and intestine, so therefore these organs are important to study. Generally speaking, the tissue-to-plasma ratios showed less pronounced differences between the strains than the absolute tissue concentrations, suggesting a strong influence of the plasma exposure. The liver-to-plasma ratio was 1.4-fold reduced in the transgenic Cyp3aXAV mice compared to *Cyp3a*$^{-/-}$ mice ($P < 0.01$, Fig. 5B, Suppl. Table 3), and there were no significant differences between wild-type and Cyp3a-deficient mice (Fig. 5B, Suppl. Table 3). The impact of CYP3A appeared to be more prominent in the small intestinal tissue-to-plasma ratios, resulting in a 1.7-fold reduction in Cyp3a deficient mice compared to wild-type ($P < 0.001$, Fig. 5C), and a 2.2-fold increase in Cyp3aXAV compared to *Cyp3a*$^{-/-}$ mice ($P < 0.0001$, Fig. 5C). This may partly reflect delayed response of the intestinal content (relative to plasma concentrations), where the recovered percentage of dose in the small intestinal tissue was only significantly different between the Cyp3a deficient mice and the transgenic CYP3A4 mice ($P < 0.001$, Fig. 5G). The spleen-to-tissue ratio was significantly enhanced in the *Cyp3a*$^{-/-}$ mice compared to wild-type ($P < 0.0001$, Fig. 5F), and reduced in Cyp3aXAV mice compared to the Cyp3a deficient mice ($P < 0.05$,

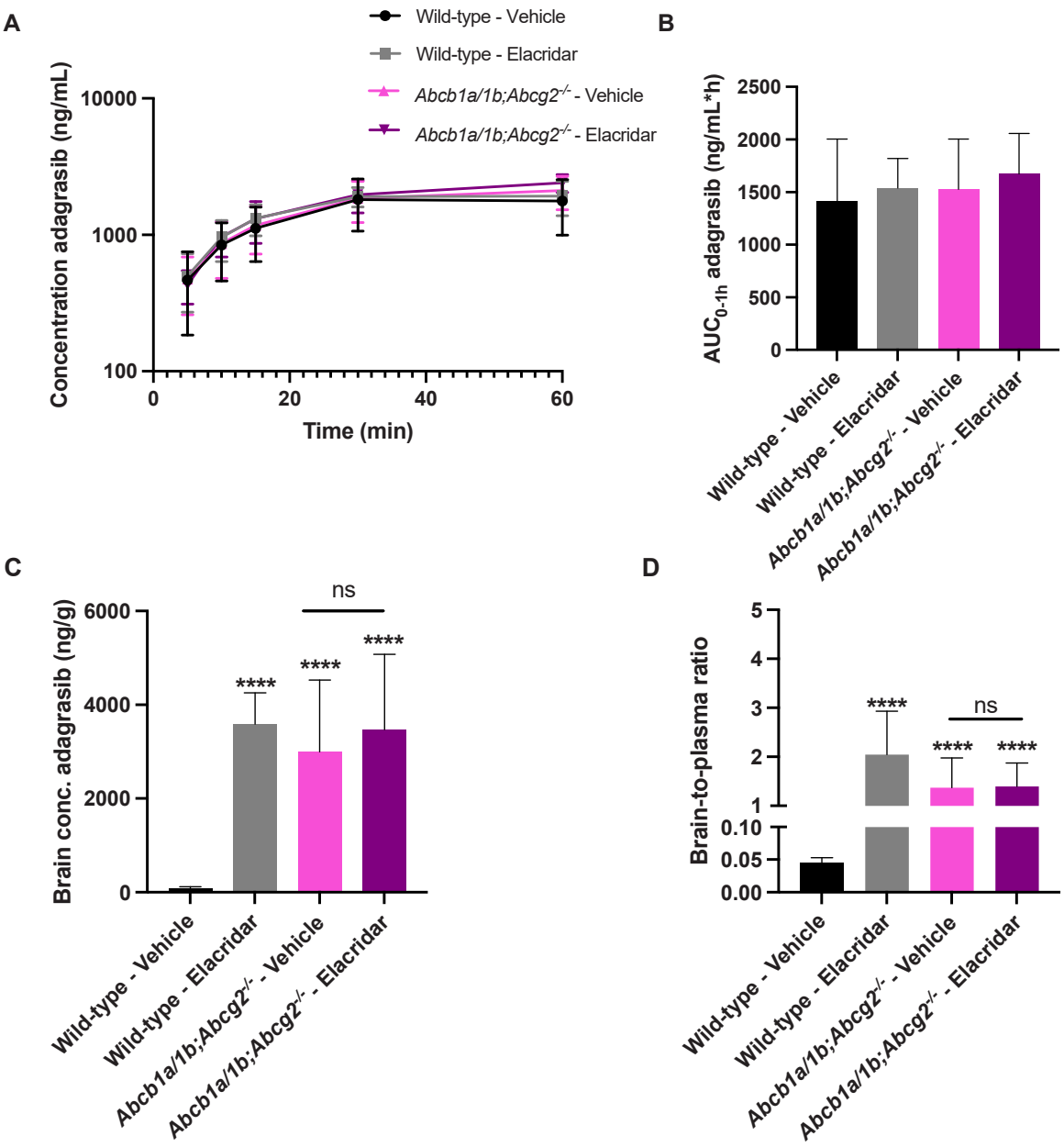

Fig. 3. Pharmacokinetic parameters of adagrasib (30 mg/kg) in female wild-type and *Abcb1a/1b;Abcg2*$^{-/-}$ mice over 1 h after oral administration and 4 h after oral administration of elacridar (50 mg/kg) or vehicle (n = 5–6). **A.** Plasma concentration time curve of adagrasib (semi-log scale). **B.** $AUC_{0-1\ h}$, area under the plasma concentration-time curve from 0 to the last time point (t = 1 h). **C.** Brain concentration (ng/g). **D.** Brain-to-plasma ratio. Data are presented as mean ± SD. Panel A: No significant differences in plasma concentration between the strains were observed at any time point. Panels B-D: ns, not significant; * ** *, $P < 0.0001$ compared to wild-type mice or another mouse strain pretreated with vehicle solution as indicated by the bars.

Fig. 5F). In the other analyzed tissues (brain, kidney, lung) only small differences in tissue disposition (when corrected for plasma exposure) were observed between these strains (Suppl. Fig. 5). In summary, these data indicate that the plasma exposure as well as the tissue disposition of adagrasib are strongly influenced by metabolism of this drug by Cyp3a and CYP3A4.

3.5. Adagrasib may be bound by plasma carboxylesterase 1c (Ces1c)

We also studied the influence of the drug-metabolizing enzyme complex Ces1 on the pharmacokinetics of adagrasib in a 2-hour experiment using wild-type and *Ces1*$^{-/-}$ mice. We observed a strong impact of the Ces1 enzyme(s) on the plasma exposure ($AUC_{0-2\ h}$ and C_{max}) of adagrasib (Fig. 6A-B, Suppl. Table 4). When compared to wild-type mice, the plasma $AUC_{0-2\ h}$ was 6.9-fold reduced in *Ces1*$^{-/-}$ mice ($P < 0.001$, Fig. 6B, Suppl. Table 4), and the C_{max} 6.5-fold (Suppl. Table 4). If adagrasib was a substrate that could be hydrolyzed by mouse Ces1, one would expect an increase in plasma levels in the *Ces1*$^{-/-}$ mice. In contrast, our results might indicate that adagrasib binds quite tightly to the abundant circulating plasma Ces1c protein in mice, resulting in increased retention. This has been observed before for a number of other drugs (such as everolimus and cabazitaxel) [29,30]. In addition, plasma retention could possibly somewhat restrict the tissue disposition of adagrasib.

Theoretically, the lower adagrasib plasma concentration observed in *Ces1*$^{-/-}$ mice might also be caused by the presence or even upregulation of some other plasma adagrasib-metabolizing enzyme in this strain, that efficiently degrades adagrasib as soon as it is no longer tightly bound to

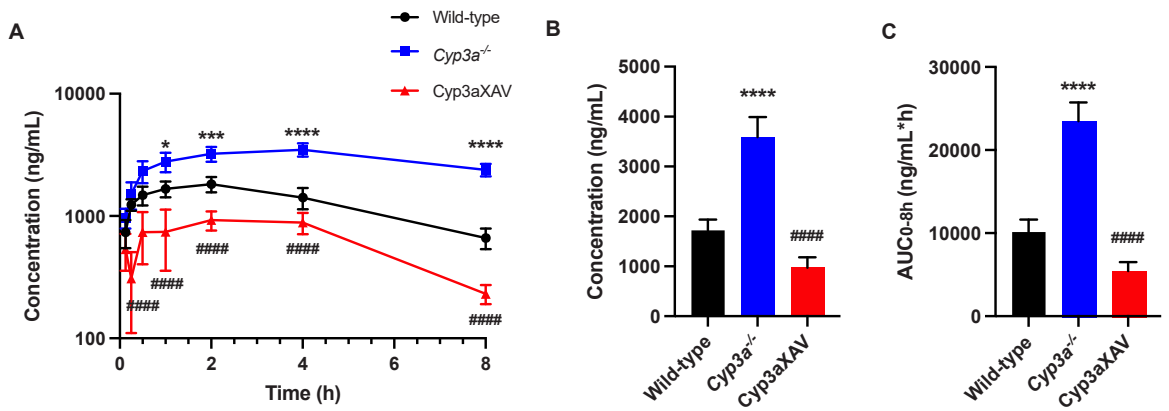

Fig. 4. Adagrasib (30 mg/kg) pharmacokinetics in female wild-type, *Cyp3a*$^{-/-}$, and Cyp3aXAV (transgenic mice with overexpression of human CYP3A4 in liver and intestine) mice over 8 h after oral administration (n = 6). **A.** Plasma concentration time curve of adagrasib (semi-log scale). **B.** C_{max}, maximum concentration of adagrasib reached in plasma. **C.** $AUC_{0-8\,h}$, area under the plasma concentration-time curve from 0 to the last time point (t = 8 h). Data are presented as mean ± SD. Panel A: * , $P < 0.05$; * ** , $P < 0.001$; * ** *, $P < 0.0001$ *Cyp3a*$^{-/-}$ compared to wild-type mice. $^{\#\#\#\#}$, $P < 0.0001$ Cyp3aXAV compared to *Cyp3a*$^{-/-}$ mice. Panels B-C: * ** *, $P < 0.0001$ compared to wild-type mice. $^{\#\#\#\#}$, $P < 0.0001$ compared to *Cyp3a*$^{-/-}$ mice.

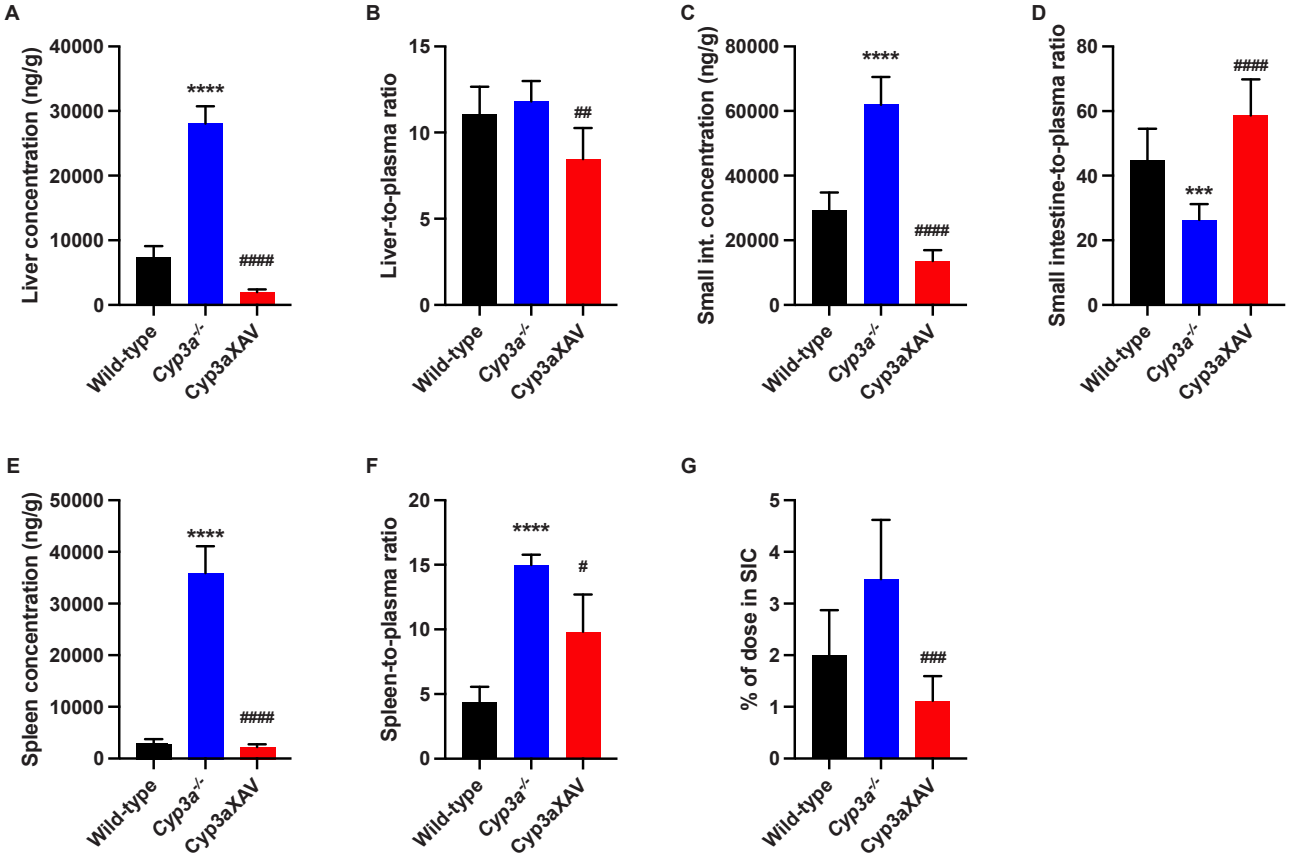

Fig. 5. Tissue distribution of adagrasib (30 mg/kg) in female wild-type, *Cyp3a*$^{-/-}$, and Cyp3aXAV mice (transgenic mice with overexpression of human CYP3A4 in liver and intestine) 8 h after oral administration (n = 6). **A.** Liver concentration. **B.** Liver-to-plasma ratio. **C.** Small intestine concentration. **D.** Small intestine-to-plasma ratio. **E.** Spleen concentration. **F.** Spleen-to-plasma ratio. **G.** Percentage of adagrasib dose recovered in small intestinal content (SIC). Data are presented as mean ± SD. * ** , $P < 0.001$; * ** *, $P < 0.0001$ compared to wild-type mice. $^{\#}$, $P < 0.05$; $^{\#\#}$, $P < 0{\cdot}01$; $^{\#\#\#}$, $P < 0.001$; $^{\#\#\#\#}$, $P < 0.0001$ compared to *Cyp3a*$^{-/-}$ mice.

plasma Ces1c. We previously observed the latter process with the drug everolimus, where even *in vitro* pre-incubation of Ces1c-proficient wild-type plasma with the generic carboxylesterase inhibitor BNPP prevented everolimus from being bound to plasma Ces1c, resulting in highly enhanced degradation of this drug in plasma [29]. To assess these possibilities, we incubated adagrasib *in vitro* with freshly collected wild-type or *Ces1*$^{-/-}$ plasma, in the presence or absence of 1 mM BNPP. Adagrasib was applied at 2000 ng/mL, close to the plasma C_{max} in wild-type mice. As can be seen from Supplemental Fig. 6, no significant degradation of adagrasib was observed in either wild-type or *Ces1*$^{-/-}$ plasma, whether in the absence or presence of BNPP. These data suggest that there is no major impact of plasma-resident adagrasib-metabolizing

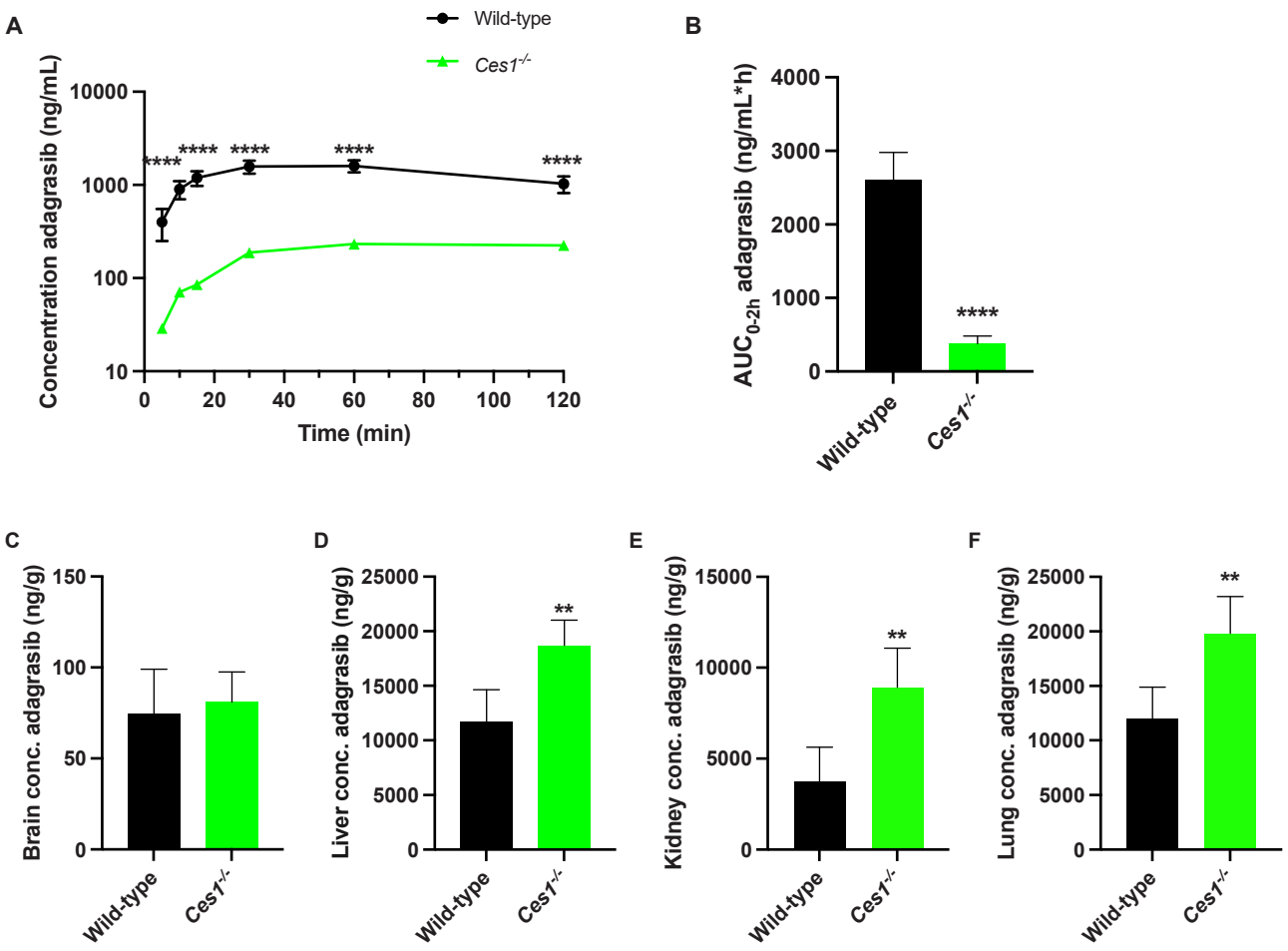

Fig. 6. Pharmacokinetic parameters of adagrasib (30 mg/kg) in female wild-type and *Ces1*$^{-/-}$ mice over 2 h after oral administration (n = 6). **A.** Plasma concentration time curve of adagrasib (semi-log scale). **B.** $AUC_{0-2\,h}$, area under the plasma concentration-time curve from 0 to the last time point (t = 2 h). **C.** Brain concentration. **D.** Liver concentration. **E.** Kidney concentration. **F.** Lung concentration. Data are presented as mean ± SD. * *, $P < 0.01$; * ** *, $P < 0.0001$ compared to wild-type mice.

enzyme(s) on the observed pharmacokinetics of adagrasib.

Due to the high impact of the Ces1 knockout on the plasma exposure of adagrasib, we did not primarily interpret tissue-to-plasma ratios, because these values are strongly driven by the altered plasma levels (Suppl. Fig. 7). Assessing the absolute tissue concentrations of adagrasib, we did observe modest increases in liver, kidney and lung in Ces1 knockout mice (Fig. 6D-F). A similar distribution pattern was observed for the spleen and small intestinal adagrasib disposition (Suppl. Fig. 7A-B). Accordingly, tissue-to-plasma ratios for these tissues were markedly increased in *Ces1*$^{-/-}$ mice by ~10-fold (data not shown). Indeed, it could be that a strongly reduced retention of adagrasib in plasma can facilitate the accumulation of adagrasib in various tissues or there could be some Ces1-mediated breakdown of adagrasib in tissue. As the only exception, the brain concentration did not seem to be influenced by absence of Ces1 (Fig. 6C). Furthermore, the percentage of dose recovered from the small intestinal content was not altered between the strains (Suppl. Fig. 7 C). Putting all of these observations together, it appears most likely that the high plasma level of adagrasib in wild-type mice is due to extensive and tight binding of adagrasib to plasma Ces1c. However, the free concentration of adagrasib in plasma was likely somewhat higher in *Ces1*$^{-/-}$ compared to wild-type mice at least part of the time, explaining the modestly increased tissue concentrations. When calculating the fraction of adagrasib retained (bound) in plasma 1 h after administration (roughly corresponding to the C_{max}), this represented at most 0.32% in wild-type versus 0.04% in *Ces1*$^{-/-}$ mice of the administered dose, assuming a total blood volume of 1.5 mL per mouse. Taking everything into account, we cannot exclude that Ces1, in addition to binding adagrasib in plasma, might also be involved in some metabolism, especially in tissues.

4. Discussion

In this study, we demonstrated that the pharmacokinetics of adagrasib is substantially affected by mAbcb1a/1b and CYP3A. Moreover, adagrasib appears to bind to plasma Ces1c in mice, whereas we cannot exclude that it is also somewhat hydrolyzed by one or more of the tissue-localized mouse Ces1 enzymes. In wild-type mice, adagrasib was rapidly absorbed with a T_{max} around 1 h, which is in agreement with an earlier mouse study describing a T_{max} of 1.5 h [1]. The observed T_{max} in wild-type mice is in line with the observed pharmacokinetic profile in humans with a median T_{max} of 4.17 h (range = 2.0–10.1 h) after a single 600 mg dose [7]. This contrasts with sotorasib, for which the T_{max} in mice (12.5 ± 3.9 min) as well as humans (~2 h) were shorter [31,32]. Another pharmacologic difference between both $KRAS^{G12C}$ inhibitors is the elimination half-life ($t_{1/2}$), which is 5 h for sotorasib compared to 23 h for adagrasib in humans. These results are in line with the observations in our mouse studies, in which the $t_{1/2}$ was 39.7 ± 3.8 min for sotorasib and 4.4 ± 0.6 h for adagrasib [7,31,32]. However, our adagrasib study has the limitation that our mice dose is relatively low compared to the human dose, when converting the 30 mg/kg for mice to a physiologically equivalent human dose [33]. Of note, this mouse study was already running by the time the first clinical data were published.

Our *in vitro* drug transport assay shows that adagrasib is effectively transported by hABCB1 and mAbcg2, but not noticeably by hABCG2. However, for the latter it is known that the expression of hABCG2 is relatively low in this cell line, which needs to be taken into account when these results are interpreted. Our results are in line with a recently published study, which showed a concentration-dependent efflux ratio of 13 in MDCK-MDR1 cells (similar to the hABCB1-overexpressing cells) [34].

The brain distribution data suggests that the brain exposure of adagrasib is mainly limited by ABCB1, because there was no difference between wild-type and *Abcg2*$^{-/-}$ mice. However, there was a significant difference between *Abcb1a/b*$^{-/-}$ and *Abcb1a/b;Abcg2*$^{-/-}$ mice, which indicates that there is a cooperative role for Abcg2 in restricting adagrasib brain distribution. Interestingly, murine Abcg2 does not seem to play a noticeable role in the pharmacokinetics of adagrasib by itself, whereas transfected-cell monolayer transport assays showed that adagrasib is a substrate for ABCG2 [8]. Therefore, the expectation is that the relative impact of ABCG2 would be more prominent in human compared to ABCB1, also because ABCG2 is relatively more abundant in the human compared to the mouse BBB [15,35].

Previously, similar transporter preferences were observed for sotorasib [31]. However, the brain penetration of adagrasib seems to be more favorable compared to that of sotorasib, because the latter had relatively low brain-to-plasma ratios of 0.02–0.03 in wild-type mice, versus 0.07 for adagrasib [31]. The higher brain disposition capacity of adagrasib (30 mg/kg) compared to sotorasib (40 mg/kg) is also reflected in the absolute brain concentrations in wild-type and *Abcb1a/1b;Abcg2*$^{-/-}$ mice, which were 139 vs. 75 ng/g in wild-type, and 6511 vs. 861 ng/g in the ABC transporter-deficient mouse strain, respectively [31]. These adagrasib results are in accordance with *in vitro* drug interaction potential studies, which showed that adagrasib is a transported substrate for both ABCB1 and ABCG2 [8]. Due to the high incidence of brain metastases in KRAS^{G12C}-mutated NSCLC of approximately 50%, this higher brain disposition of adagrasib might be therapeutically beneficial [18]. *In vivo* (mouse model) brain penetration experiments showed time- and dose-dependent penetration of adagrasib in the CNS. Furthermore, nearly complete saturation of ABCB1-dependent efflux was observed in the BBB at a mouse dose of 200 mg/kg (comparable with the human 600 mg twice daily dose), which is 6.7-fold higher than the 30 mg/kg used in this study [34]. At this 200 mg/kg dose, sufficient brain penetration of adagrasib could be reached to treat potential brain metastases [34]. In patients with CNS metastasis, the objective response rate is 33.3% (n = 33), although it is recommended to treat these patients prior with radiotherapy [8,36].

In addition, we showed that significant improvement of the brain penetration of adagrasib without saturation of the efflux transporters at the BBB can also be achieved by coadministration of the dual ABCB1/ABCG2 inhibitor elacridar, resulting in complete inhibition of the ABC transporters at the BBB. The inhibitory effects of elacridar were more prominent for the brain disposition of adagrasib compared to sotorasib, resulting in an approximately 44- vs. 13-fold increase in brain concentrations, and 56- vs. 8-fold increase in brain-to-plasma ratios, respectively [31]. These results further support that adagrasib is a more potent substrate of the (mouse) ABC transporters in comparison to sotorasib. No signs of acute CNS toxicity of adagrasib were observed in the Abcb1a/1b- and/or Abcg2-deficient mouse strains or mice treated with elacridar, in contrast to some other TKIs such as brigatinib, which resulted in lethal toxicity in *Abcb1a/1b;Abcg2*$^{-/-}$ mice [37]. Although elacridar is still under clinical investigation for human application, it seems that it is well tolerated in humans [38]. As adagrasib at the current clinical dose (600 mg b.i.d.) may perhaps reach high enough trough levels to obtain sufficient brain penetration, possibly elacridar could be used to lower the adagrasib dose, thereby saving costs and unnecessary systemic exposure to higher doses.

Highly effective ABCB1 inhibitors could alter the pharmacokinetics of adagrasib, but it has also been shown that adagrasib is an inhibitor of ABCB1 itself. Adagrasib has a reported IC_{50} of 592 ng/mL for ABCB1 inhibition, possibly leading to a concentration-dependent inhibition of its own efflux as well [34]. Adagrasib might prevent ATP from binding to ABCB1, thereby restricting its efflux pump function [39]. As a transported substrate, it might also simply saturate the transport activity of ABCB1 at higher concentrations. However, this inhibition of ABCB1 does not seem to fully affect the transport of adagrasib, based on the efflux ratio of 13 reported for the MDCK-ABCB1-overexpressing cell line at a concentration of 2 μM adagrasib, which is twice the IC_{50} value. This means that adagrasib may alter the pharmacokinetics of other ABCB1 substrate drugs, including coadministered anticancer drugs. Therefore, combination therapy of adagrasib and other drugs that are also affected by ABCB1 should be applied with caution.

Moreover, tumors (over-)expressing ABCB1 might show intrinsic or acquired resistance against adagrasib. During adagrasib treatment, some KRAS^{G12C} tumors could increase the expression level of ABCB1, resulting in resistance to adagrasib, in addition to other types of acquired resistance [39–43]. The expression level of ABCB1 in lung tumor cells is normally relatively low, but previous exposure to chemotherapy could result in increased expression levels and eventually lead to acquired drug resistance [44,45]. For example, NSCLC patients previously treated with cisplatin showed upregulation of both ABCB1 and ABCG2 [46]. Due to the different resistance mechanisms, probably the best treatment regimen is a combinatorial therapy of a KRAS^{G12C} inhibitor, such as sotorasib or adagrasib, with immunotherapy, as pembrolizumab (in NSCLC) or cetuximab (in colorectal cancer), which will improve their efficacy [47–49]. On the other hand, a study of Zhang et al. demonstrated *in vitro* as well as *in vivo* (mouse models) that addition of adagrasib to other anticancer drugs could overcome multidrug resistance in chemotherapy, which is probably related to the ABCB1 inhibitory potency of adagrasib [39].

Furthermore, the plasma pharmacokinetics of adagrasib were significantly enhanced in *Cyp3a*$^{-/-}$ mice and reduced in the transgenic Cyp3aXAV mice, indicating that adagrasib is a good substrate for this metabolizing enzyme. Therefore, CYP3A4 will probably have a significant role in the oral availability and metabolism of adagrasib in patients. The overall plasma and tissue exposure to adagrasib was markedly lower in the transgenic CYP3A4 mouse strain, which is probably due to higher expression of human CYP3A4 in the liver and intestine or to higher efficiency of human CYP3A4 in the metabolism of adagrasib compared to murine Cyp3a. Compared to sotorasib, adagrasib seems to be a similarly affected substrate of CYP3A4, with a 3.9-fold (sotorasib) versus 4.3-fold (adagrasib) decrease in plasma exposure in transgenic Cyp3aXAV mice compared to *Cyp3a*$^{-/-}$ mice [31]. *In vitro* human liver hepatocytes studies showed that the majority of the hepatic oxidative metabolism of adagrasib is regulated by CYP2C8 (28%) and CYP3A4 (72%). Interestingly, these studies also showed that adagrasib is an inhibitor of CYP2B6, − 2C9, and − 3A4. For the latter, adagrasib was a time-dependent inhibitor [8]. Based on these results in combination with our results, coadministration of CYP3A4 inducers or inhibitors might alter the systemic exposure to adagrasib. Combinations of such coadministered drugs should therefore be applied with caution.

Moreover, the plasma exposure of adagrasib was also affected by the Ces1 enzyme resulting in significantly lower plasma levels in the Ces1-deficient mouse strain compared to wild-type mice. In addition, the absolute tissue concentrations were somewhat enhanced by knocking-out the carboxylesterase 1 enzyme. This suggests that adagrasib binds to plasma Ces1c in mice and it might be possible that it is a somewhat hydrolyzed substrate of one or more of the tissue-localized Ces1 enzymes as well. However, Ces1c is highly abundant in mouse plasma, but CES1 in humans is not, so there will be no direct implication for the clinical application of adagrasib [25].

5. Conclusion

In vivo adagrasib is a strong substrate for the efflux transporter

ABCB1 and the drug-metabolizing enzyme CYP3A4. Additionally, adagrasib binds to mouse plasma Ces1c and is perhaps a hydrolyzed substrate of tissue-localized Ces1 enzymes. Adagrasib brain penetration is highly restricted by ABCB1, in combination with ABCG2. Their influences in the BBB can be completely reversed by the addition of the booster elacridar, which dramatically increases the brain penetration without any signs of acute CNS toxicity in wild-type mice. Based on our study, it is suggested that CYP3A4 polymorphisms or coadministration of strong inducers and/or inhibitors of CYP3A4 and P-gp (ABCB1) could potentially alter the systemic exposure of adagrasib, including the brain penetration of the drug. The latter is especially important for the treatment of brain (micro-)metastases. The results obtained from this study could be useful for further improvement of the safety and efficacy of adagrasib, when using this drug in the clinic.

Funding source

This research did not receive any specific grant from funding agencies in the public, commercial, or not-for-profit sectors. Part of this research was funded by core funding of the Netherlands Cancer Institute.

CRediT authorship contribution statement

Nancy H.C. Loos: Conceptualization, Formal analysis, Investigation, Methodology, Visualization, Writing – original draft. **Irene A. Retmana:** Sample bioanalysis, Visualization, Writing – review & editing. **Jamie Rijmers:** Contribution in performing transwell experiment and mouse experiments pilot study, Writing – review & editing. **Yaogeng Wang:** Contribution in performing mouse experiments pilot study, Writing – review & editing. **Changpei Gan:** Contribution in development of *Ces1*$^{-/-}$ mouse strain, Writing – review & editing. **Maria C. Lebre:** Contributed the reagents, materials, and mice, Writing – review & editing. **Rolf W. Sparidans:** Supervision of bioanalytical analysis, Writing – review & editing. **Jos H. Beijnen:** Supervision, Writing – review content. **Alfred H. Schinkel:** Conceptualization, Supervision, Formal analysis, Writing – review & editing. All authors commented on and approved the manuscript.

Declaration of Competing Interest

The research group of A.H. Schinkel receives revenue from commercial distribution of some of the mouse strains used in this study. The other authors have nothing to declare related to this study.

Data Availability

The data that supports the findings of this study are available in the supplementary material of this article.

Appendix A. Supporting information

Supplementary data associated with this article can be found in the online version at doi:10.1016/j.biopha.2023.115304.

References

[1] J.B. Fell, et al., Identification of the clinical development candidate MRTX849, a covalent KRAS(G12C) inhibitor for the treatment of cancer, J. Med. Chem. 63 (13) (2020) 6679–6693.
[2] J. Hallin, et al., The KRAS(G12C) inhibitor MRTX849 provides insight toward therapeutic susceptibility of KRAS-mutant cancers in mouse models and patients, Cancer Discov. 10 (1) (2020) 54–71.
[3] L. Huang, et al., KRAS mutation: from undruggable to druggable in cancer, Signal Transduct. Target Ther. 6 (1) (2021) 386.
[4] H.A. Blair, *Sotorasib: First Approv.* Drugs 81 13 2021 1573 1579.
[5] F. Skoulidis, et al., Sotorasib for lung cancers with KRAS p.G12C mutation, New Engl. J. Med. 384 (25) (2021) 2371–2381.
[6] FDA, U.S.F.a.D.A. *Prescribing information Krazati*^{TM} (adagrasib). 2022 [cited 2023 10–2-2023]; Available from: ⟨https://www.accessdata.fda.gov/drugsatfda_docs/label/2022/216340s000lbl.pdf⟩.
[7] S.I. Ou, et al., First-in-human phase I/IB dose-finding study of adagrasib (MRTX849) in patients with advanced KRAS(G12C) solid tumors (KRYSTAL-1), J. Clin. Oncol. 40 (23) (2022) 2530–2538.
[8] P.A. Jänne, et al., Adagrasib in non-small-cell lung cancer harboring a KRAS(G12C) mutation, New Engl. J. Med. 387 (2) (2022) 120–131.
[9] F. Oesch, Importance of knowledge on drug metabolism for the safe use of drugs in humans, Drug Metab. Rev. 41 (3) (2009) 298–300.
[10] K.M. Giacomini, et al., Membrane transporters in drug development, Nat. Rev. Drug Discov. 9 (3) (2010) 215–236.
[11] A.H. Schinkel, J.W. Jonker, Mammalian drug efflux transporters of the ATP binding cassette (ABC) family: an overview, Adv. Drug Deliv. Rev. 55 (1) (2003) 3–29.
[12] S. Choudhuri, C.D. Klaassen, Structure, function, expression, genomic organization, and single nucleotide polymorphisms of human ABCB1 (MDR1), ABCC (MRP), and ABCG2 (BCRP) efflux transporters, Int. J. Toxicol. 25 (4) (2006) 231–259.
[13] D.S. Miller, ABC transporter regulation by signaling at the blood-brain barrier: relevance to pharmacology, Adv. Pharm. 71 (2014) 1–24.
[14] S.C. Tang, et al., Impact of P-glycoprotein (ABCB1) and breast cancer resistance protein (ABCG2) gene dosage on plasma pharmacokinetics and brain accumulation of dasatinib, sorafenib, and sunitinib, J. Pharm. Exp. Ther. 346 (3) (2013) 486–494.
[15] X. Bao, et al., Protein expression and functional relevance of efflux and uptake drug transporters at the blood-brain barrier of human brain and glioblastoma, Clin. Pharm. Ther. 107 (5) (2020) 1116–1127.
[16] A.H. Schinkel, et al., P-glycoprotein in the blood-brain barrier of mice influences the brain penetration and pharmacological activity of many drugs, J. Clin. Investug. 97 (11) (1996) 2517–2524.
[17] J. Goncalves, et al., Relevance of breast cancer resistance protein to brain distribution and central acting drugs: a pharmacokinetic perspective, Curr. Drug Metab. 19 (12) (2018) 1021–1041.
[18] P. Tomasini, et al., EGFR and KRAS mutations predict the incidence and outcome of brain metastases in non-small cell lung cancer, Int. J. Mol. Sci. 17 (12) (2016) 2132.
[19] G. Szakács, et al., The role of ABC transporters in drug absorption, distribution, metabolism, excretion and toxicity (ADME-Tox), Drug Discov. Today 13 (9–10) (2008) 379–393.
[20] O. Lolodi, et al., Differential regulation of CYP3A4 and CYP3A5 and its implication in drug discovery, Curr. Drug Metab. 18 (12) (2017) 1095–1105.
[21] U.M. Zanger, M. Schwab, Cytochrome P450 enzymes in drug metabolism: regulation of gene expression, enzyme activities, and impact of genetic variation, Pharm. Ther. 138 (1) (2013) 103–141.
[22] J.K. Lamba, et al., Genetic contribution to variable human CYP3A-mediated metabolism, Adv. Drug Deliv. Rev. 54 (10) (2002) 1271–1294.
[23] D. Wang, et al., Human carboxylesterases: a comprehensive review, Acta Pharm. Sin. B 8 (5) (2018) 699–712.
[24] Q. Jin, et al., Optical substrates for drug-metabolizing enzymes: Recent advances and future perspectives, Acta Pharm. Sin. B 12 (3) (2022) 1068–1099.
[25] R.D. Jones, et al., Carboxylesterases are uniquely expressed among tissues and regulated by nuclear hormone receptors in the mouse, Drug Metab. Dispos. 41 (1) (2013) 40–49.
[26] R. Evers, et al., Drug export activity of the human canalicular multispecific organic anion transporter in polarized kidney MDCK cells expressing cMOAT (MRP2) cDNA, J. Clin. Investig. 101 (7) (1998) 1310–1319.
[27] B. Poller, et al., Double-transduced MDCKII cells to study human P-glycoprotein (ABCB1) and breast cancer resistance protein (ABCG2) interplay in drug transport across the blood-brain barrier, Mol. Pharm. 8 (2) (2011) 571–582.
[28] J.W. Jonker, et al., Role of breast cancer resistance protein in the bioavailability and fetal penetration of topotecan, J. Natl. Cancer Inst. 92 (20) (2000) 1651–1656.
[29] S.C. Tang, et al., P-glycoprotein, CYP3A, and plasma carboxylesterase determine brain and blood disposition of the mTOR Inhibitor everolimus (Afinitor) in mice, Clin. Cancer Res. 20 (12) (2014) 3133–3145.
[30] S.C. Tang, et al., P-glycoprotein, CYP3A, and plasma carboxylesterase determine brain disposition and oral availability of the novel taxane cabazitaxel (Jevtana) in mice, Mol. Pharm. 12 (10) (2015) 3714–3723.
[31] N.H.C. Loos, et al., ABCB1 limits brain exposure of the KRAS(G12C) inhibitor sotorasib, whereas ABCB1, CYP3A, and possibly OATP1a/1b restrict its oral availability, Pharm. Res. 178 (2022), 106137.
[32] D.S. Hong, et al., KRAS(G12C) inhibition with sotorasib in advanced solid tumors, New Engl. J. Med. 383 (13) (2020) 1207–1217.
[33] A.B. Nair, S. Jacob, A simple practice guide for dose conversion between animals and human, J. Basic Clin. Pharm. 7 (2) (2016) 27–31.
[34] J.K. Sabari, et al., Activity of adagrasib (MRTX849) in brain metastases: preclinical models and clinical data from patients with KRASG12C-mutant non-small cell lung cancer, Clin. Cancer Res. 28 (15) (2022) 3318–3328.
[35] X. Liu, ABC family transporters, Adv. Exp. Med. Biol. 1141 (2019) 13–100.
[36] P.A. Jänne, J.K. Sabari, A.I. Spira, Adagrasib in non-small-cell lung cancer. Reply, New Engl. J. Med. 387 (13) (2022) 1238–1239.
[37] W. Li, et al., P-glycoprotein and breast cancer resistance protein restrict brigatinib brain accumulation and toxicity, and, alongside CYP3A, limit its oral availability, Pharm. Res. 137 (2018) 47–55.
[38] R.P. Dash, R. Jayachandra Babu, N.R. Srinivas, Therapeutic potential and utility of elacridar with respect to P-glycoprotein inhibition: an insight from the published in

vitro, preclinical and clinical studies, Eur. J. Drug Metab. Pharm. 42 (6) (2017) 915–933.
[39] Y. Zhang, et al., Adagrasib, a KRAS G12C inhibitor, reverses the multidrug resistance mediated by ABCB1 in vitro and in vivo, Cell Commun. Signal. 20 (1) (2022) 142.
[40] V. Dunnett-Kane, et al., Mechanisms of resistance to KRAS(G12C) inhibitors, Cancers 13 (1) (2021) 151.
[41] M.M. Awad, et al., Acquired resistance to KRAS(G12C) Inhibition in Cancer, New Engl. J. Med 384 (25) (2021) 2382–2393.
[42] N.S. Akhave, A.B. Biter, D.S. Hong, Mechanisms of resistance to KRAS(G12C)-targeted therapy, Cancer Discov. 11 (6) (2021) 1345–1352.
[43] T. Koga, et al., KRAS secondary mutations that confer acquired resistance to KRAS G12C inhibitors, sotorasib and adagrasib, and overcoming strategies: insights from in vitro experiments, J. Thorac. Oncol. 16 (8) (2021) 1321–1332.
[44] I. Zawadzka, et al., The impact of ABCB1 gene polymorphism and its expression on non-small-cell lung cancer development, progression and therapy - preliminary report, Sci. Rep. 10 (1) (2020) 6188.
[45] D. Campa, et al., A comprehensive study of polymorphisms in ABCB1, ABCC2 and ABCG2 and lung cancer chemotherapy response and prognosis, Int. J. Cancer 131 (12) (2012) 2920–2928.
[46] M. Vesel, et al., ABCB1 and ABCG2 drug transporters are differentially expressed in non-small cell lung cancers (NSCLC) and expression is modified by cisplatin treatment via altered Wnt signaling, Respir. Res. 18 (1) (2017) 52.
[47] E. Corral de la Fuente, et al., Targeting KRAS in non-small cell lung cancer, Front. Oncol. 11 (2021), 792635.
[48] Frontline Promise for Adagrasib-Pembrolizumab Combination Cancer Discov. 13 2 2023 Of2.
[49] R. Yaeger, et al., Adagrasib with or without cetuximab in colorectal cancer with mutated KRAS G12C, New Engl. J. Med. 388 (1) (2023) 44–54.